NAIC-ID(RS)T-0705-94

NATIONAL AIR INTELLIGENCE CENTER

PROPAGATION AND TRANSFORMATION PROPERTIES OF AXICON OPTICAL SYSTEMS FOR LASER BEAMS

by

Cai Bangwei, Lu Baida, et al.

Approved for public release;
Distribution unlimited.

HUMAN TRANSLATION

NAIC-ID(RS)T-0705-94 15 December 1994

MICROFICHE NR: 94C000565

PROPAGATION AND TRANSFORMATION PROPERTIES OF AXICON OPTICAL SYSTEMS FOR LASER BEAMS

By: Cai Bangwei, Lu Baida, et al.

English pages: 12

Source: Zhongguo Jiguang, Vol. A21, Nr. 1, January 1994; pp. 21-25

Country of origin: China
Translated by: Leo Kanner Associates
F33657-88-D-2188
Quality Control: Nancy L. Burns
Requester: NAIC/TATD/Bruce Armstrong

GRAPHICS DISCLAIMER

All figures, graphics, tables, equations, etc. merged into this translation were extracted from the best quality copy available.

STOP HERE

L

PROPAGATION AND TRANSFORMATION PROPERTIES OF AXICON OPTICAL SYSTEMS FOR LASER BEAMS

Cai Bangwei, Lu Baida, Zhang Bin, Feng Guoying and Wang Bihua; Cai, Lu, Zhang and Feng of Department of Optoelectronics, Sichuan University, Chengdu 610064; Wang of Zigong Institute of Chemical Engineering Research and Design, Zigong 643000

Abstract:

Axicon optical systems can transform a gaussian beam into a diffraction-free Bessel beam. In addition, mutual transformation between solid beam and annular beam can also be realized. The paper details theoretical analyses and experimental studies on the axicon and its composite optical system; both results are in agreement. Axicon optical systems are shown to have wide applications in laser techniques.

Key words: axicon beam converters, diffraction-free Bessel beam, annular beam

I. Introduction

With laser processing and the rapid development of the nonsteady-state laser cavity, high-energy tubular laser devices, and X-ray laser devices, it becomes necessary to transmit and transform laser beam on a customized basis. For example, a solid-core transverse-cross-section light beam is transformed

into an annular beam, a plane or diametral slender ring-shaped focusing light beam, and vice versa. Or, a gaussian light beam is transformed into a diffraction-free Bessel beam, among other possibilities. Obviously, these purposes are not possible with conventional spherical-surface-system light beam converters. J. H. Mcleod was the first researcher to introduce the simple concept of the imaging properties of axicon; however, the concept of a "diffraction-free" Bessel beam [1] was not proposed at the time. In the paper, the authors quantitatively analyzed the parametric relation using the axicon as the light beam converter. In addition, the transmission and transformation properties of He-Ne and CO_2 lasers were experimentally verified with a light-beam converter fabricated by the authors. As their results showed, the axicon optical system can accomplish light beam transmission and transformation in multiple forms with a high transformation efficiency. The axicon optical systems have very attractive application values in laser boring, as well as heat treatment, welding and slicing of cylindrical workpieces, in addition to the high-precision collimation technique.

II. Focusing Properties of the Axicon

Because it passes through the transverse cross-section of the axial line while displaying a biprism pattern, the axicon is also called an axial prism; this is a cone-shaped optical component. In this paper, we refer to it, briefly, as a pyramid lens with the convergence and divergence functions of a light beam. However, its focusing property differs from that of the spherical-surface lens. Fig. 1(a) shows the transverse cross-section of a positive axicon: the z-axis is the optical axis; emitted from point light source S on the axis, light passed through the axicon; after refraction, the light beam intersects the z-axis at the isogonal angle δ.

Based on the law of refraction, the deviated angle of the refracted light relative to incident light is

$$\delta = 2\sin^{-1}[n\sin(\varphi/2)] - \varphi \qquad (1)$$

When ϕ is very small ($\varphi < 0.17$ rad), there is

$$L' = \frac{Ltgu}{tg(\delta - u)} = \frac{Ltgu'}{tg[(n-1)\varphi - u]} \qquad (2)$$

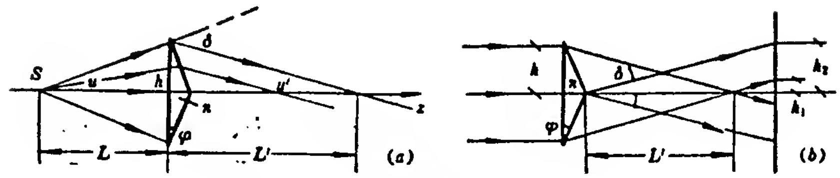

Fig. 1 Focusing properties of positive axicon

In the equation, n is the refractivity of the material of which the pyramid lens is made; ϕ is its prism angle; L is the distance to object; u is the diametral angle of a square hole in the object; u' is the diametral angle of a square hole in the image; and L' is the distance to the image. As revealed by Eq. 2, for the same diametral angle u of square hole in the object for the same point light source, the light ray produces a single focus on the z-axis after passing through a positive axicon. After passing through a positive axicon, all light rays with different u-angles have foci on the z-axis; the infinite-number of foci generate a fine continuous line that overlaps with the z-axis.

As shown in Fig. 1(b), after passing through a positive axicon, all the refracted light rays of parallel light beams with radius h intersect with the z-axis; even so, a continuous focal line is formed. When ϕ is very small, the length of the focal line (neglecting the thickness of the positive axicon) is

$$L' = h/[(n-1)\varphi] \qquad (3)$$

The maximum length of the focal line is

$$L_{max}' = h_{max}/[(n-1)\varphi] \qquad (4)$$

Obviously, the larger the light passage aperture h, and the smaller prism angle ϕ, the longer is the focal line. Within the

focusing zone L'_{max}, interference is produced due to mutual overlapping of emitted light rays, thus forming a long, slender focusing light field. In addition, within the large range of collimation, there is still a relatively high density of light power, thus capable of being used as a dye laser device, as a pumping light in an X-ray laser device, and as a laser beam for drilling deep hole. For field distribution within L'_{max}, by solving the wave equation

$$[\nabla^2 - (1/c^2)(\partial^2/\partial t^2)]E(r,t) = 0 \tag{5}$$

we derive [2]

$$E(r,t) = J_0(\alpha r)\exp[i(\beta z - \omega t)] \tag{6}$$

Eq. (6) is a special solution of Eq. (5); in the equation, ∇ is the Laplacian operator; r is the positional coordinate; t is time; and J_0 is the zero-order Bessel function, $r^2 = x^2 + y^2, \alpha^2 + \beta^2 = (\omega/c)^2 = k^2$. Obviously, the oscillation amplitude portion in Eq. 6 is a function only of r and is not related to coordinate z in the propagation direction. In other words, within L'_{max} in the range of the Bessel light zone, the light intensity perpendicular to the transverse plane of the z-axis does not vary with change in propagation distance. This phenomenon is called the "diffraction-free" property; the light beam is called a diffraction-free Bessel light beam [3, 4]. As shown in numerical calculations, when the value of z approaches L'_{max}, the light intensity at the transverse plane varies with oscillation.

Based on the property of the Bessel function, we can obtain the diameter of the central light spot of the light beam

$$D = 4.81/\alpha = 4.81\lambda/[2\pi(n-1)\varphi] \tag{7}$$

In the equation, λ is wavelength of incident light. When $z>L'_{max}$, the emitted light beams do not overlap, thus forming a divergent annular light beam. The size of the ring increases as z is made larger; the width of the ring is

$$\Delta h = z\mathrm{tg}\delta - (z - L')\mathrm{tg}\delta \approx h_{max} \tag{8}$$

During the transmission process, the ring width remains unchanged and is equal to the radius of the incident parallel light beam.

As parallel light beams pass through a negative pyramid lens, the light beams diverge as they deviate from the optical axis at an equal angle δ, and are transformed into an annular light beam as shown in Fig. 2. In the figure, ø is the conical angle; D is depth of cone; for the ring, the outer diameter $: h_2 = (L' - D)\mathrm{tg}\delta + h$, and the inner diameter $h_1 = L'\mathrm{tg}\delta$. When ø is very small and if we neglect the thickness of the pyramid lens, the width of the annular light beam is

$$\Delta h = h - D(n - 1)\varphi \approx h \tag{9}$$

Δh is related only to the diameter of incident light beam and to the parameters of the pyramid lens, but is not related to the transmission distance z. The ring width is still a constant.

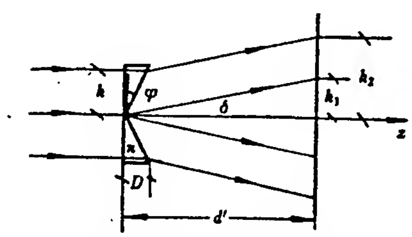

Fig. 2 Negative transmitting axicon

III. Pyramid Lens Composite System

As shown in Fig. 3, by combining a positive and a negative pyramid lens with the same prism angle ø, a new pattern expander of annular light beams can be constituted.

After a parallel light beam passes through this composite system, the light beam can be transformed into a collimated annular light beam. Conversely, the collimated annular light beam can be transformed into a solid-core parallel light beam. By adjusting the spacing d between the positive and the negative pyramid lens, the ring diameter of the emitted light beam can be made to vary continuously; however, the ring width still remains constant. It is easy to verify that the relation between the amplifying rate and the parameter of the composite system can be expressed as

$$M = 1 + (d\varphi/h)(n-1) \qquad \varphi < 0.17 \text{ rad} \qquad (10)$$

When d=0 and M=1, there is no amplification power for the composite system; the function is the same as for a conventional optical window. If d is made larger, the amplification power becomes larger. M_{max} is limited by the aperture of the output positive pyramid lens; from Eq. 10, we can determine the maximum d. For the composite system, energy losses are very small during the light beam transformation process. The system can be applied to transform an annular light beam (outputted from a nonsteady-state cavity laser device or from a tubular-shaped solid laser device) into a solid-core parallel light beam, and can be used as a beam expander of a high-energy tubular-shaped solid laser amplifing system.

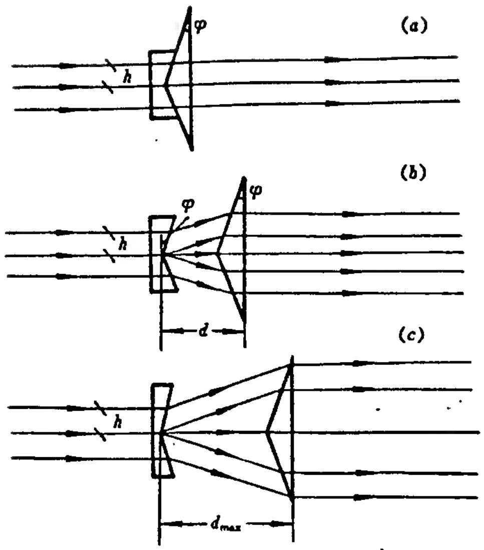

Fig. 3 The axicon beam expander

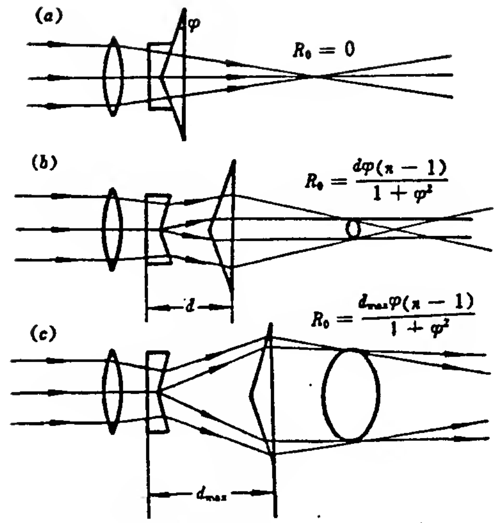

Fig. 1 Changing ring diameters by combining a lens and axicon

If a spherical-surface positive lens is added to this composite system, its application range can be further expanded. As shown in Fig. 4, the composite system can transform a solid-core parallel light beam into a slender ring. The radius of the focusing ring is determined by the following equation.

$$R_0 = [d\varphi(n-1)]/(1+\varphi^2) \qquad (\varphi < 0.17\ \mathrm{rad}) \qquad (11)$$

In the equation, d is the spacing between the positive and the negative pyramid lens; ϕ is the prism angle. By changing d, the magnitude of R_0 can be randomly adjusted. When d=0, R_0=0. At the maximum value R_{max}, R_0 is limited by the aperture of the positive pyramid lens, thus corresponding to maximum d_{max}. In the techniques of laser boring, cutting, welding, and heat treatment of annular workpieces, if the light beam transform device is adopted as shown in Fig. 4, direct processing on large-diameter workpieces is feasible without moving the focusing laser beam, or without moving the workpiece. Hence, expensive laser scanning

devices, rotary work platforms, and other precision machines are not required; in addition, adjustments can be made to the ring aperture (for processing) ranging from micrometers to centimeters.

IV. Experimental Results

Fig. 5 shows an experimental set-up for determining the light-beam transform property of the pyramid lens.

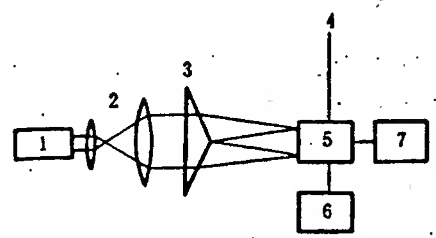

Fig. 5 Experimental arrangement
1 — laser; 2 — expander; 3 — axicon; 4 — screen
5 — detector; 6 — scanning driver; 7 — recorder

For a 10mW He-Ne laser beam with its beam expanded by a telescope, after a collimated parallel light beam of 2h in diameter is obtained, the beam is directed orthogonally incident onto the pyramid lens to be determined, and a line-focusing light beam and annular light beam are obtained. By using optical screen 4 or detector 5, the optical-spot dimension and light-intensity distribution are measured, respectively.

4.1. Measuring the focusing parameter of a positive pyramid lens

The positive pyramid lens used was designed and machined by

authors of this paper. ϕ=50 mm; the material is K_9 glass (or KCl crystal); the prism angle $\phi=5.3^0$; the diameter (of the collimated parallel light beam) 2h=39 mm. By moving the optical screen to directly accept the light spot of the transformed light beam, observation confirms the presence of equal-intensity light spots at any transverse cross-section within the range from vertex O to L'_{max}. From Eq. 4, calculate the maximum length (of the focusing line) L'_{max}=391mm; the experimentally determined value is 378mm. For light-intensity distribution between 0 and approximately L'_{max}, the small-aperture scanning method is used in making measurements; the small-aperture diameter is 26 micrometers. The axicon is placed in front of detector 5 silicon photocell (3DU33); a synchronous electric motor drives the precise guide-rail threaded rod to perform transverse-direction scanning along the vertical optical axis. Fig. 6 shows the light-intensity distribution on the transverse plane at L=105mm; the optical power density of the central bright spot is very high. The experimental curve (a) is in general agreement with the numerical calculated curve (b).

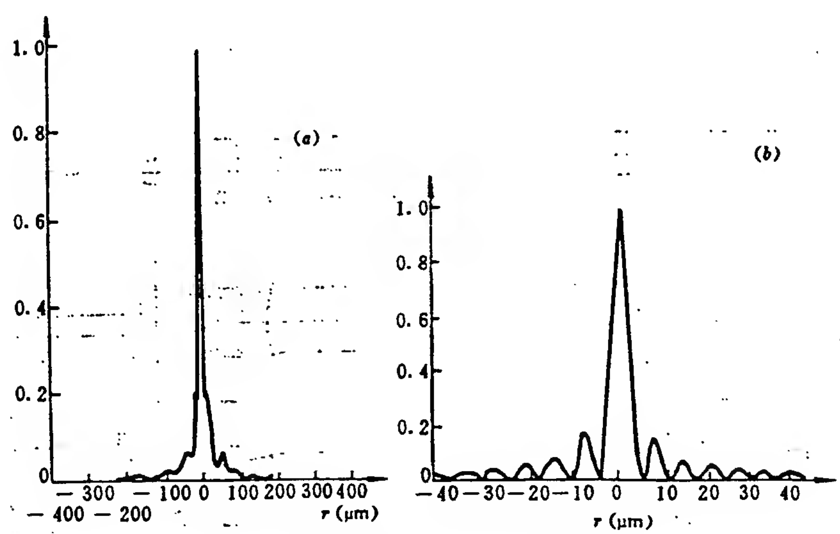

Fig. 6 Intensity distributions of Bessel beam

(a) Experimental beam profile; (b) Calculated beam profile

Fig. 7 shows the variation rule of axial light intensity $I(I \propto EE^{*})$ with L' within the range of L'_{max}. When $L' < 350\,\mathrm{mm}$, the light-intensity distribution on the transverse plane remains basically unchanged. When L' approaches L'_{max}, the light-intensity oscillation rapidly increases. The curve in Fig. 7 is the result of numerical calculation. The experimentally determined values are shown with circular dots; both (experimental and calculated) values are in basic agreement. Thus, it is verified that the light-intensity distribution within the Bessel light zone is not related to the transmission distance z, with the "diffraction-free" property.

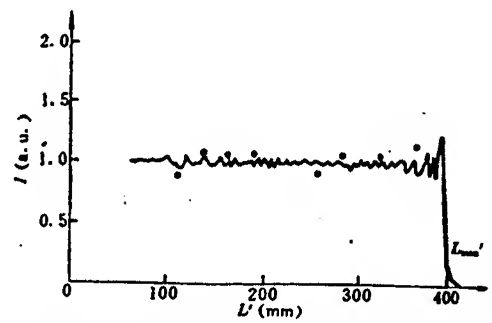

Fig. 7 The axial intensity I of Bessel beam as a function of distance

When λ=0.6328 micrometer, by calculating using Eq. 7, the dimension (of the central bright spot) is $D_{Theory} = 10.2\,\mu m$. After calibration on the transverse-direction scanning distance, with multiple measured values at different positions, $D_{Exp.} = 14.5 \pm 1.0\,\mu m = \bar{D} + a_{0}\bar{D}$ is the mean value; a is the root-mean-square deviation. As shown by the measurements, the dimension of the central optical spot generally does not change; long, slender focusing is realized within the Bessel light zone.

4.2. Measurement of transform efficiency

By using a laser wattmeter, measure the laser power before and after transformation through a pyramid lens; thus, the

transform efficiency, $\eta = 84.7\%$ of the pyramid light-beam transform device (without an antireflection coating film) is obtained. After a coating with antireflection film, transform efficiency η can be greater than 92 percent.

4.3. Measurement of annular light beam

When one places the light screen outside L'_{max}, the focusing bright spot disappears, and the annular light beam is continuously received. To increase z continuously, the ring diameter increases, but the ring width stays constant, as shown in Fig. 8(a). The measured ring width is 18.5mm, which is basically consistent with the theoretical calculated value of 19.5mm.

By using a negative pyramid lens in experiments, similar results of maintaining the width of the annular light beam can be achieved.

In Fig. 8(b), a photograph of a slender ring (on the focal plane) is obtained as the parallel light beam passes through the composite optical system transform device as shown in Fig. 4. By changing the spacing d between the positive and the negative pyramid lenses, the ring diameter can be continuously changed as required.

One can extend the above-mentioned experiment to the infrared range and use a CO_2 laser as the light source; the same result can also be obtained by using a zinc selenide lens beam expander for beam expansion along with orthoincident to KCl crystal pyramid lens. Fig. 8(c) shows a circular ring picture as ablated on a wooden board by an infrared laser.

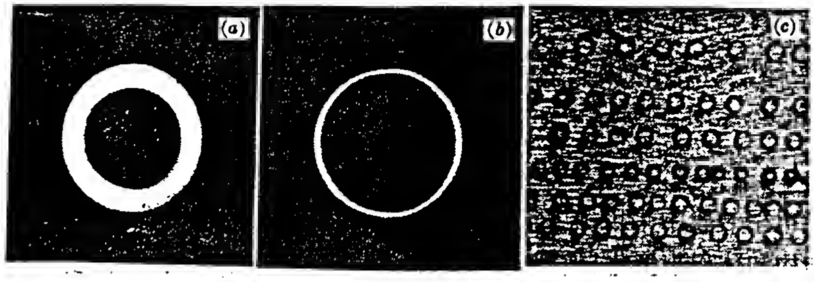

Fig. 8
(a) annular beam; (b) annular focusing beam; (c) burned rings by CW CO_2 at wood plate

The research was funded by the Zigong Municipal Science Commission. The first draft of the article was received on 6 April 1993; the final, revised draft was received on 20 May 1993.

REFERENCES

1 J. H. Mcleod. *J. Opt. Soc. Am.*, 1954, 44: 592
2 J. Durnin *et al.*. *J. Opt. Soc. Am.*, 1987, A4: 651
3 J. Durnin *et al.*. *Appl. Opt.*, 1988, 27: 3959

4. Lu Baida, et al, GUANGXUE XUEBAO [JOURNAL OF OPTICS], 1993, 13(9), page 840.

DISTRIBUTION LIST

DISTRIBUTION DIRECT TO RECIPIENT

ORGANIZATION	MICROFICHE
B085 DIA/RTS-2FI	1
C509 BALLOC509 BALLISTIC RES LAB	1
C510 R&T LABS/AVEADCOM	1
C513 ARRADCOM	1
C535 AVRADCOM/TSARCOM	1
C539 TRASANA	1
Q592 FSTC	4
Q619 MSIC REDSTONE	1
Q008 NTIC	1
Q043 AFMIC-IS	1
E051 HQ USAF/INET	1
E404 AEDC/DOF	1
E408 AFWL	1
E410 AFDTC/IN	1
E429 SD/IND	1
P005 DOE/ISA/DDI	1
P050 CIA/OCR/ADD/SD	2
1051 AFIT/LDE	1
P090 NSA/CDB	1
2206 FSL	1

Microfiche Nbr: FTD94C000565
NAIC-ID(RS)T-0705-94